

Master in Photonics

MASTER THESIS WORK

ROBUST MODULAR OPTICAL BIOSENSORS

Feroz Ahmed

Supervised by Dr. Mauricio Moreno Sereno, Francisco Palacio (UB)

Presented on date 9th September 2013

Registered at



Escola Tècnica Superior
d'Enginyeria de Telecomunicació de Barcelona

Robust Modular Optical Biosensors

Feroz Ahmed, Dr. Mauricio Moreno Sereno, Francisco Palacio

Laboratory 224: Integrated Optics and Optoelectronics, Department of Electronics, University of Barcelona, C. de Martí i Franquès 1, Barcelona 08028, Spain.

E-mail: feroz.ahmed.eee@gmail.com

Abstract Optical Waveguide Light Spectroscopy (OWLS) is a type of label-free technique of optical biosensing. It is based on the coupling of laser light in an optical waveguide through a Diffraction Grating (DG) fabricated in the surface. The coupling angle is related with the instantaneous refractive index or thickness of a bio-layer growing over the DG.

Thinking in multiple measurements simultaneously in this work, we present the design of electronic board and electronic control of a commercial array of 512 photo-detectors with a microcontroller. The array will be used for monitoring the output of multiple laser beams from the edge of an optical grating waveguide sensor. Data from the array are transferred using a USB cable to a Personal Computer for drawing and processing.

Keywords: Linear array photodetectors, Evanescent field, Diffraction grating, Optical biosensors.

1. Introduction to Bio-sensors:

1.1. Optical Bio-sensor.

A biosensor is an analytical device consisting on three individual parts: (i) an immobilized biological sensitive material, which roles the recognition element (enzyme, antibody, antigen, organelles, DNA etc.) integrated within a (ii) physicochemical transducer and (iii) an electronic part. The transducer converts the bio-logical information into a quantitatively measureable signal usually in the form of optical, acoustic, electrical or magnetic response [1]. According to the most typical transducers used in biosensors, they are classified as (a) Non-optical: Piezo-electric biosensors (effects due to the mass of the reactants or products), potentiometric biosensors (changes in the distribution of charges causing an electrical potential to be measured), amperometric biosensors (movement of electrons produced in a redox [reduction-oxidation] reaction), impedance biosensors (change in the electrical impedance of an interface in AC steady state with constant DC bias conditions), and (b) optical: Fluorescence, absorbance, luminescence biosensors (light output during the bio-recognition reaction or light absorbance difference between the reactants and products), evanescent wave sensors etc [2].

Optical waveguides are the basic element of evanescent bio-sensors. An optical waveguide is formed by a core layer of material of certain refractive index surrounded by two other media with lower refractive indices. Light is confined within the core layer by successive total internal reflections at the core-cladding media interfaces. Although light travels confined within the core layer, there is a part of the guided light travelling through a region that extends outside, around hundred of nano-meters, into the media surrounding the waveguide: this is the evanescent field. When there is a change in the optical characteristics of the outer medium (i.e. refractive index change), a modification in the propagation of the light (phase velocity) is induced via the evanescent field. Different types of evanescent biosensors are: optical fibers, resonant mirror, Surface Plasmon Resonance (SPR), Mach-Zender interferometer and grating coupler biosensors. All these techniques are also known as label free optical biosensors [2].

One of the most relevant evanescent optical biosensor is the SPR which is a physical process that can occur when monochromatic TM [transversal magnetic] polarized light hits a metal film; generally gold [3]. Usually all the incoming light is reflected by the metal layer, but in the resonant condition at an specific angle, the electric field of the incoming light put to oscillate the electrons of the metal layer and the light is not reflected; this detection method is called angular interrogation [4,6]. Also it is possible to illuminate with white light and measuring the non-reflected wavelength; in this case this method is called spectral interrogation [5,6].

1.2. Optical Grating Coupler Bio-sensors (OGCB):

An OGCB is based on a diffraction grating patterned on the surface of a waveguide. When the light is incident at a specific or resonant angle on the grating, the light can couple into the thin optical waveguide. The resonant or coupling condition relies on the following equation:

$$\pm N_{\text{eff}} = n_{\text{cover}} \sin \alpha + m \frac{\lambda}{\Lambda} \quad (\text{i})$$

where: N_{eff} = Effective index of the sandwich layers; m diffraction order, λ wavelength of laser, Λ grating period and α coupling angle. Typically grating period is less than the used wavelength; for example: $\Lambda=500\text{nm}$. In figure 1-Right, we described this type of waveguide bio-sensor.

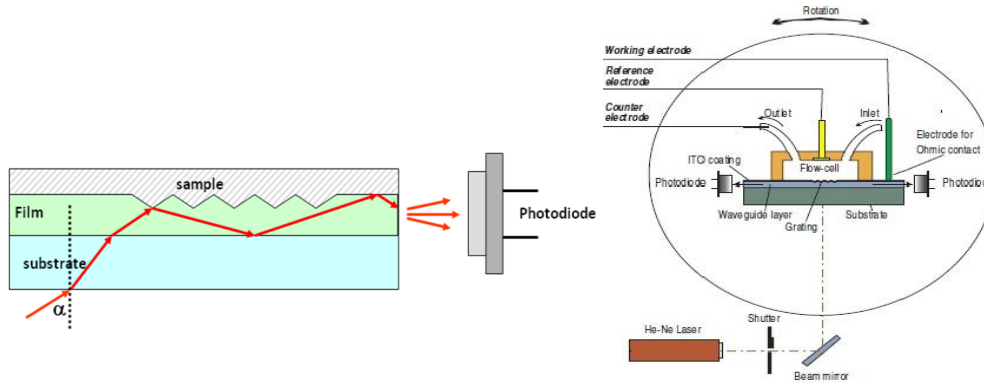


Figure 1: Left: Grating couples the laser into the waveguide at a well-defined angle, and the in-coupled light is captured by the detector.

Right: Description of the components in an OWLS instrument. A flow through the flow cell serves for the controlled exchange of analytes.

The coupled light can be detected at the end of the waveguide with a photodiode. This technique is also known as OWLS. By using the physics of a diffraction grating, OGCB measures the concentration of an analyte by detecting changes in the angle at which light couples into a waveguide. Biological receptors on the surface of the waveguide capture the molecules of interest, which affect bio-layer's thickness and refractive index seen by the evanescent wave. Continuously measuring the shift of these coupling angles allows the direct online monitoring of the kinetics of the reaction. OGCB can be included to the label-free techniques [7, 8].

There is a commercial instrument based on the above principle, Micro-vacuum®, Figure 1-Right [9]. The performance of this commercial system can be improved if we could do multiple measurements simultaneously. In Figure 2 Left, we present an optical chip with several diffraction gratings fabricated on the surface. The waveguide is a Si_3N_4 dielectric layer of 90nm thickness on a silica substrate. Each grating has $300\mu\text{m} \times 300\mu\text{m}$ area, with a period of $\Lambda=500\text{nm}$ and an etching depth of 30nm. In Figure 2 right, several laser beams (6 in the photograph) are coupled simultaneously [10].

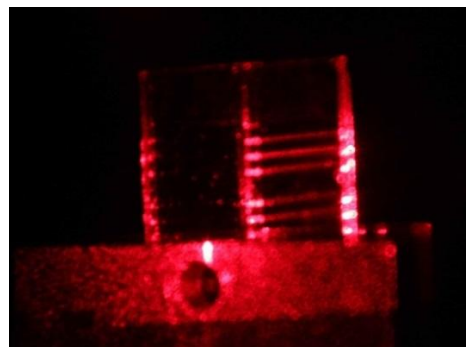
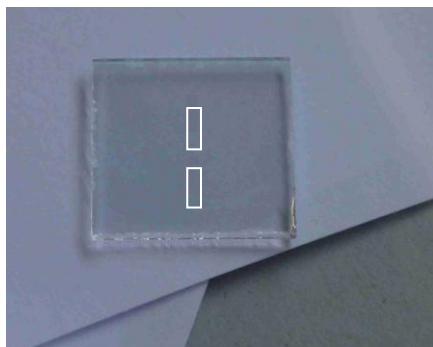


Figure 2 Left: Optical Grating: four gratings in each rectangle. Chip size = $1.5\text{cm} \times 1.5\text{cm}$.

Right: Example of simultaneous coupling in an array of diffraction for multi-analyte

2. Objectives:

Our starting point is the coupling light in an optical sensor with only a diffraction grating and two photodiodes [9]. All the system is controlled with LABVIEW [10].

For reading simultaneously the multiple out-coupled beams in the edge of the sensor, we need multiple detectors, but this is not practical. That is why, from technical point of view, it is necessary an integrated array of photo-detectors.

In our work, we used the Hamamatsu S3922, characterized by a length of 10 mm and 512 numbers of pixels. For in-coupling the light from He-Ne laser beam simultaneously in all diffraction gratings, it's necessary to use a cylindrical lens [10].

Our objective is the programming of control signals of this sensor, the sensor data acquisition with a microcontroller, and transfer data to a personal computer for visualization and processing.

3. Hardware Engineering

In this part, overview of main components of the system and the connections between them are described in detail.

3.1. Optoelectronic Sensor:

The Hamamatsu S3922 is a linear image sensor designed for spectrophotometry and 1D image acquisition; figure 3-Left depicts the sensor. It has been selected for the detection of several laser beams in our prototype. It is a linear array of 512 pixels; each one has a large active area with a pixel pitch of $25\mu\text{m}$ and pixel height of $500\mu\text{m}$, also, it is highly sensitive in the UV region. The image sensor consists of a scanning circuit made up of MOS transistors, a photodiode array, and a switching transistor array that addresses each photodiode, all integrated onto a monolithic silicon chip. The output waveform can be read out with a simple external circuit, as can be seen at Figure 3-Right, or directly with any Analog to Digital Converter (ADC) depending on the applications [11].

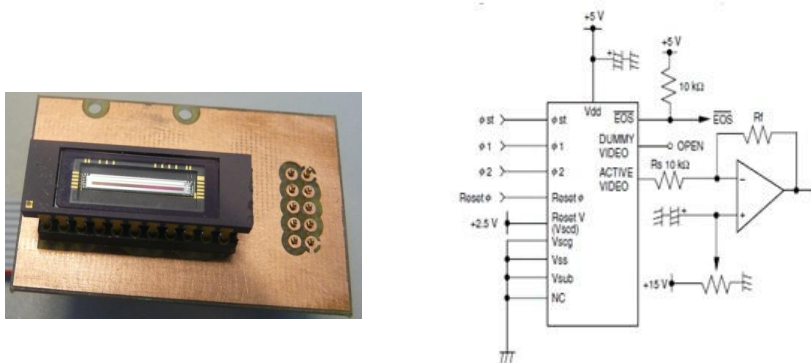


Figure 3: Left: Image of Hamamatsu S3922 linear sensor; Right: Readout circuit proposed by Hamamatsu

The photodiode array operates in charge integration mode, which means that the output is proportional to the amount of light exposure (light intensity \times integration time). Other features are a low power consumption of 10 mW and 5V single power supply operation. The output voltage in the Active Video pin goes from 2.5V to 0V. This voltage is related to the Reset V terminal that needs to be supplied for an external fixed (2.5V) [11].

3.1.1. Sensor signals:

To drive the sensor is required three clock pulses; (ϕ_1, ϕ_2 and ϕ_{st}). These pulses are compatible with 5V CMOS logic. The scanning circuit and the switching transistor of the sensor are

controlled by the signals ϕ_1 and ϕ_2 . That allows the reading of each pixel sequentially. These signals can be generated independently and must be complementary; both pulses must not be high at the same time. The shift register starts the scanning at the 'high' level of ϕ_{st} . The timing chart for the drive circuit and the sequential video output is described in figure 4 [11].

In figure 5-left the timing sequence diagram is shown. From top to down colored signals are start (yellow), ϕ_1 (green), $RESET$ (violet) and output (pink). The integration time is defined by the low state of $RESET$ signal as we can see by the inserted white lines. The slope in the output [pink color] is the integration of photo generated current. When $RESET$ goes high, the output goes to 2.5V. In figure 5-right, we see the colored signals ϕ_{st} (yellow) and output (green). The total output corresponds to 512 pixels of array of photo-detectors when a laser beam is focused on the sensor.

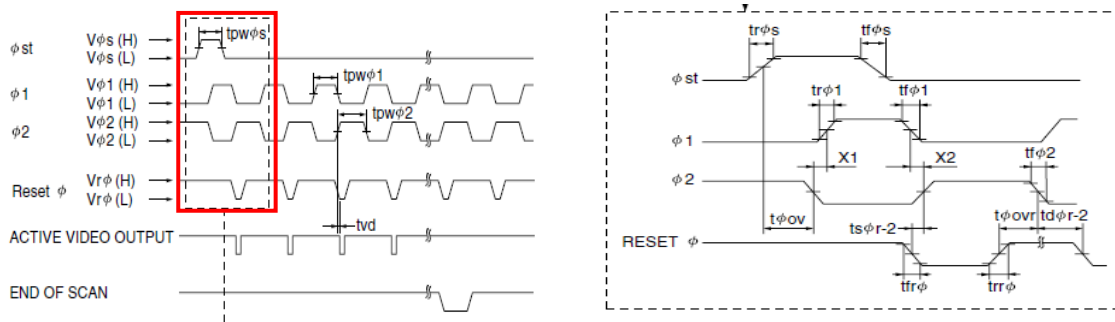


Figure 4: Left: Timing chart for the driver circuit; Right: Details of $\phi_1, \phi_2, \phi_{st}$ and $RESET$

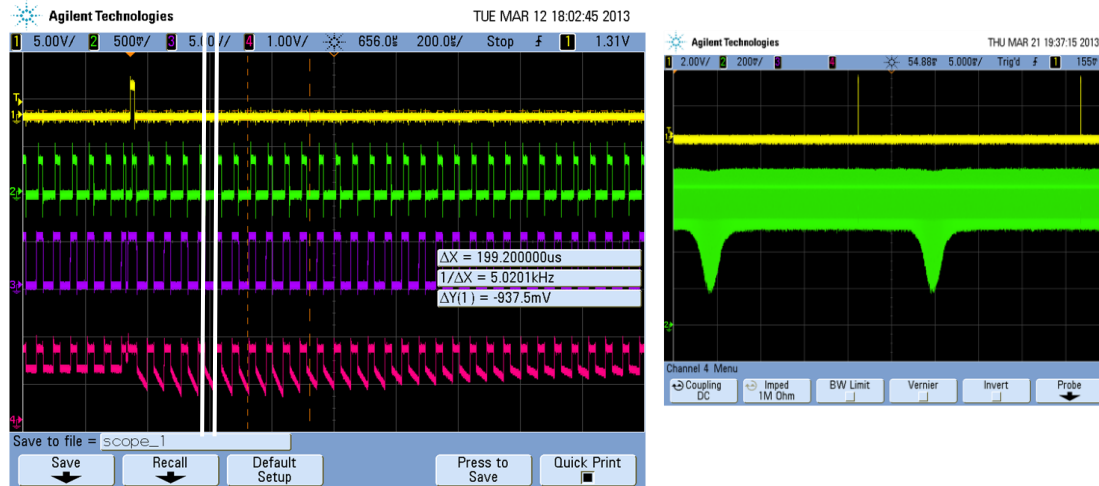


Figure 5: Left: Timing signals and output of the sensor. White lines define the integration time. Right: ϕ_{st} and Video output of array of photo-detectors.

3.2. The Microcontroller

A Microcontroller (μC) is a small computer on a single integrated circuit, including a processor, memory, and programmable input/output peripherals. Controlling the signals and acquisition of the output waveform of the Hamamatsu S3922 and transferred data to the Personal Computer (PC) for processing and visualization have to be done with a μC .

There are several microcontroller families in the market (For example: Texas, Freescale, Intel etc.). In our project, Microchip® has been selected because of the previous experience on programming this family in the Department of Electronics. The selected microcontroller is PIC 24HJ128GP502, a 16-bit μC whose operating range is up to 40 MIPS operation, and biasing at 3.0-3.6V. It has 128 bytes of programmable flash memory, 2 UARTs for communication with PC or peripherals, and one 10 bits Analog to Digital Converter (ADC) [12].

This μC has been selected because it is implemented in the Microstick[®] board. This board includes an integrated debugger/programmer, a socket for the device under test and pins that facilitate insertion into a prototyping board for extremely flexible development [12]. All these features are done using a common USB cable. Also it includes a connector for a serial communication based on the TTL-232R-3V3 cable [13].

3.3. System Description/Implementation:

The entire system consists of two boards, one used as a μC pins extension and the other used as a sensor holder. Both boards are connected by a 10 lines flat cable, this hardware separation has been decided because the sensor has a reduced space inside of the experimental setup. The boards have been implemented with the help of the DesignSpark[®] software. Figure 6- Left shows the μC board and figure 6-Right shows the sensor board.

The μC board has an extension of the μC pins in order to facilitate the connection of test probes. It includes the 10 pin connector to be connected to the sensor board and the generation of the 2.5V, using a symmetric voltage divider resistors of same value, in this case 10K Ω , needed for the Reset V terminal of the sensor, Figure 7- Left.

The sensor board has been designed following the specific dimensions needed to fit the sensor in the experimental setup. This board includes the 22 pin sensor socket and the 10 pins connector to be connected to the μC board.

The system voltage is supplied by the computer using the USB. Using this power source the prototype becomes more flexible and cheap, avoiding then the need of an external power source.

3.3.1. μC and Sensor connections:

The control signals $\phi_1, \phi_2, \phi_{st}$ and RESET from suitable pins of sensor are connected to the corresponding pins of the μC . Due to the different working voltage, 3.3V for the μC and 5V for the sensor, these pins have been configured as a Open Drain Configuration (ODC) using pull-up:

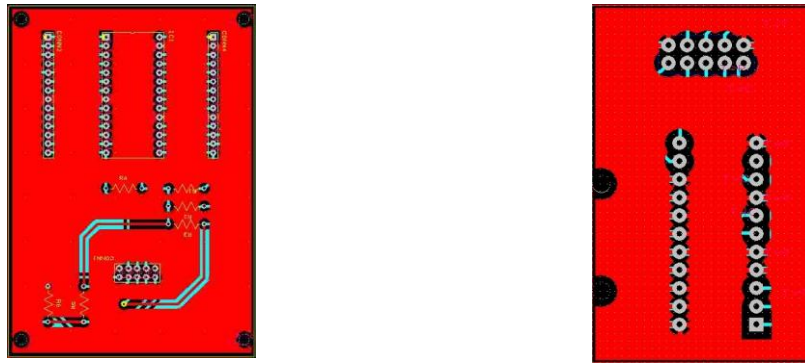
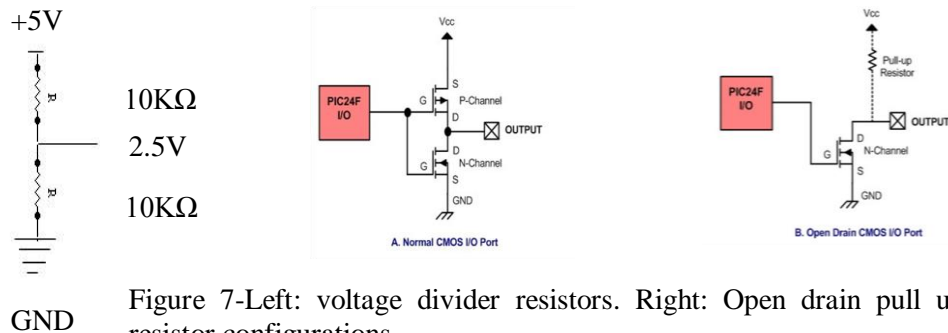


Figure 6: Photographs of the developed PCB showing the μC part for programming, communication (Left) and sensor control (Right).



The analog Video output signal has to be digitalized for transmit and analyze the sensor data. It is done using an ADC. As commented before, the selected μC has already implemented internally a 10 bits ADC. So, the sensor output is connected to one of the specific ADC pin of the μC and the 2.5V is connected to another specific ADC pin of the μC [12]. The ADC has been configured to perform a differential conversion between these two pins, that means that the result will be $V_{ADC} = 2.5V - V_{OUTPUT}$. This configuration prevents future operations and provides a better resolution. Finally, in Figure 7, it is described all features mentioned above.

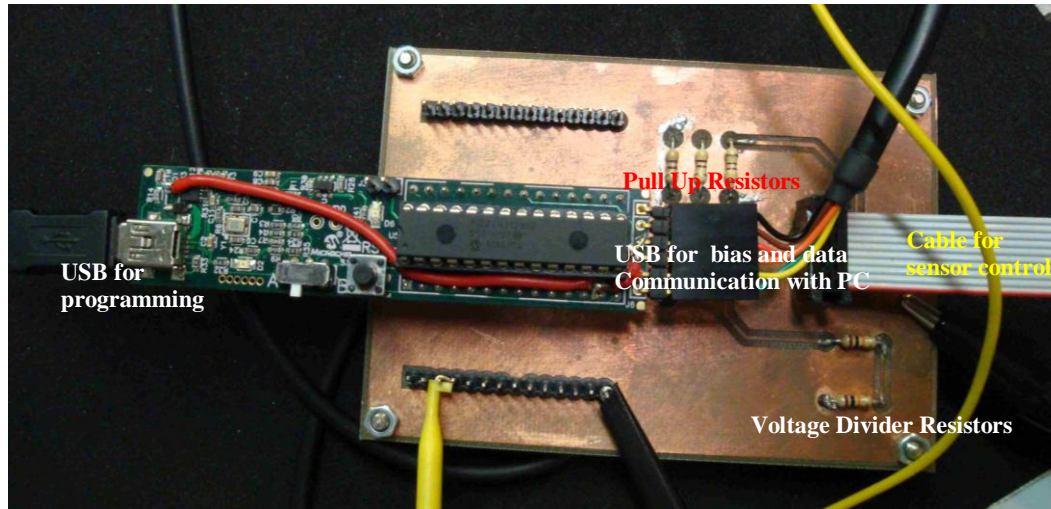


Figure 7: Photograph of the developed PCB showing the cables for programming, communication and sensor control.

3.3.2. Connection between μC and PC:

TTL-232R-3V3 is a USB to serial converter cable which provide connectivity between USB connectors in the PC and serial UART interface in the μC working at 3.3V. It is used for serial communication between PC and μC and supplying power to the whole hardware system from the PC, so, the system doesn't require any external power supply [13].

For this, some modifications on the μC kit have been made. These have been achieved by connecting the Vcc of cable to the Vcc = 5V of the Microstick ®. It is done with the red cable which is shown in Figure 7.

4. Software Engineering.

In this part, overview of programming of the system is described in detail.

4.1. Microcontroller program flow diagram:

In Figure 8, it is described the flow diagram of μC program which consists of 3 blocks.

(i) It begins with **initialization block**:

- Definition of the clock of the system.
- Declaration of the type of Input-Output (I/O) pins.
- Configuration of the UART: 1-stop bit, no parity, 8-data bits and bit rate of 115200 bps.
- Configuration of the Open Drain Collector (ODC).
- Configuration of the ADC.

(ii) In the second block, μC waits to receive the integration time from the PC.

(iii) In the last block, μC reads the output of the sensor continuously. Inside this block, the main tasks are:

- Generation of the start pulse.
- Generation of the control signals.

- Calling to ADC and at the end of the integration time.
- The last three processes are repeated 512 times, the number of pixels of array.
- Transmission to the PC of 512 pixels data using 2 bytes for each pixel. The reason is that ADC is 10 bits and serial transmission of data is 8 bits.

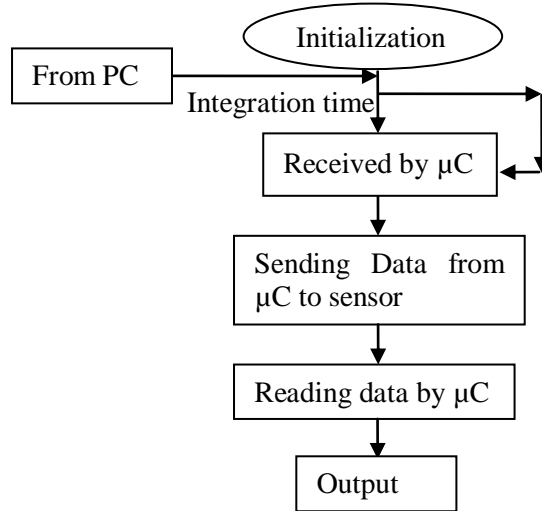


Figure 8, Flow Diagram of μ C from PC to sensor to read output data.

4.2 Matlab program flow diagram:

In Figure 9 Left, it is represented the Matlab Graphical User Interface(GUI) to show some control buttons for interrupting /initiating the data transmission and reception process towards the μ C.

- **Initialization** step is taken for creating Matlab Figure.
- By pressing '**CONNECT**' button, serial data communication starts. That communication can be set from the following features of μ C: 1-stop bit selection, no parity selection, 8-data bits and bit rate of 115200 bps for speed control of data, compatible Port Number selection.
- '**Port Number**' activates specific port number for opening serial communication towards μ C from PC. In our case, it is always COM 4.
- The variation of range of integration time from 2ms to 100ms is controlled by a slider tool of Matlab. Instantaneous changing of slider to fix a specific time represents Intensity vs Pixel Number curve in the upper portion of graph in Figure. At the same time, lower portion graph indicates the evolution in time of the more illuminated pixel when there is only one laser beam coupled.
- '**DATA ACQUISITION**' button is initiated for sending data from PC to μ C and received data by the μ C. The fact is that with these sending and received data towards μ C, each integration time for the scanning of 512 pixels of data at each time is activated within the Data Acquisition process. Every time the process is repeated by changing the integration time up to 100ms maximum range. The position of Maximum Illuminated Pixel (MIP) at each scanning time up to 512 pixels is set to watch the output in the second graph from the Data Acquisition control. Data Acquisition control is set for writing the data for digital output and evolution of sensor.
- '**LOAD DATA**' actually starts the desired data loaded from the computer to the μ C. That is, digital output and evolution of sensor are configured appropriately to display in the GUI with graphical views.
- Finally, for each data transmission and reception process, another push button '**STOP**' is used to finish each task.

Figure 9, Right presents the flow diagram of Matlab program.

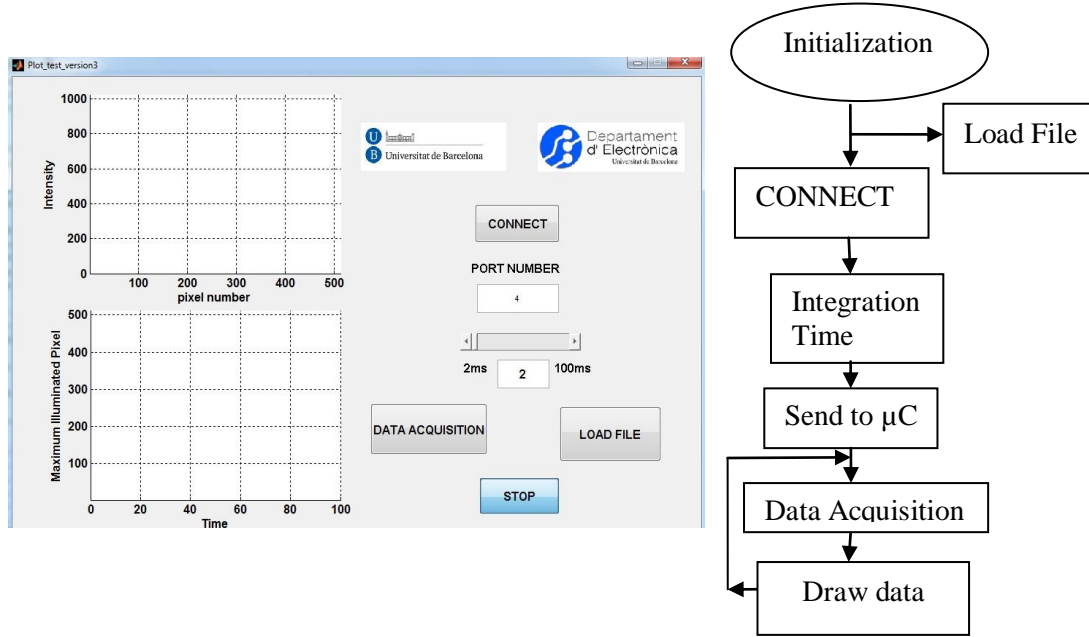


Figure 9, Left: Representation of GUI interface to control the transmission and reception process of μC from PC. Right: Flow diagram of Matlab Program

5. Result

Figure 10 shows the digital output of the sensor with different integration times. It has been obtained from a focused laser approximately in the center of the array. The time indicated in the graph is defined as the whole reading time of the sensor and range from 2ms to 100ms. The impact of integration times is observed in the amplitude of the detected signals. It is found that with the increase of integration time, the amplitude of peaks become large gradually. In this particular example, above 20ms, saturated outputs are given by the sensor.

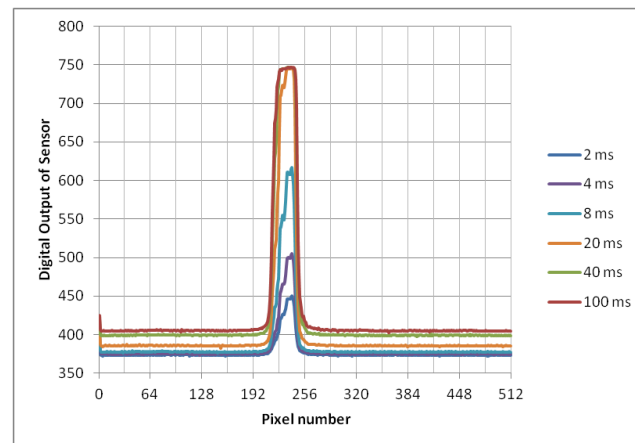


Figure 10: Digital Output of Sensor vs. Pixel number curve to show output response of sensor

The Figure 11-Left shows the flow cell containing the optical sensor. An He-Ne laser is focused in the center of the chip with a convergent lens (focal length of 10cm), and the light is coupled when the angle between the normal to the surface of the sensor and He-Ne laser is 10° . Also, it is seen the output of the beam at the edge of the sensor. Figure 11-right shows the said flow cell with the attached PCB containing the array of photo detectors. The coupling angle is found with manual rotation of the base of the mechanical structure.

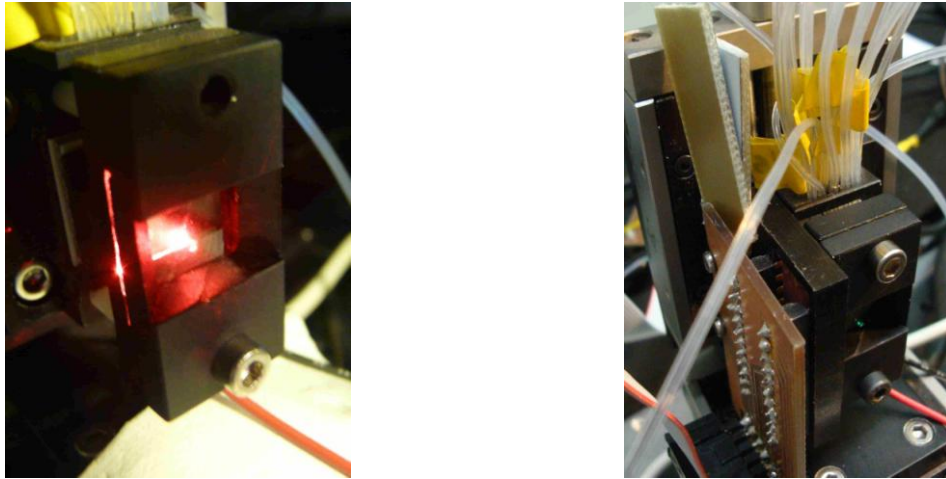


Figure 11- Left: Output of the coupled beam at the edge of sensor.
Right: Flow cell with the attached PCB of the array of photo detectors.

Figure 12-Left, shows the capture by the array of photo-detectors of multiple (in this case, 4) laser beams at the edge of the sensor. In this case, a cylindrical lens is placed after the He-Ne laser that generates a line (a line of gratings are aligned with an array of photo detectors) on the array of grating in the optical sensor, as described before in Figure 2.

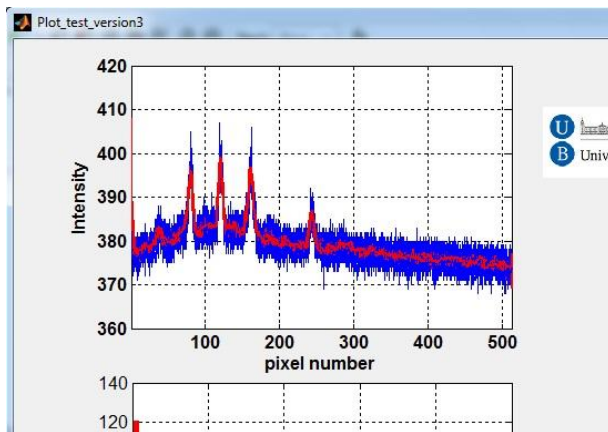


Figure 12-Left: Multiple output beams displayed as a Matlab output.
Right: Appearance of those beam spots from experimental result obtained in Lab.

6. Conclusion:

In this project, we have programmed PIC24HJ128GP microcontroller for controlling a linear array of 512 photo detectors, with the goal of monitoring multiple incident laser beams on the optoelectronic sensor.

With the Analog-to-Digital conversion and data transmission features of the μC , the profile of incident laser beams has been transferred to a Computer for Visualization and future processing in a MATLAB environment.

Test of the optoelectronic sensor under near real operation conditions has been done: laser light from a He-Ne laser source has coupled within the optical grating coupler chip with appropriate incident angle. Reading of the multiple laser beams coupled has been successfully visualized in the computer.

7. Future work:

Several of future tasks are:

- Programming the stepper motor in Matlab through another serial port and synchronization with the reading of the array of photo detectors.
- Checking the compatibility of all needed USB ports of PC working in different environments.
- Processing output sensor for tracking more than one laser beam with appropriate coupling angles.
- Use of liquids with different refractive indices in order to characterize the sensitivity of the system: Change in the coupling angle in front of change in the refractive index.
- All these tasks are needed for robust instruments for future Bio-medical measurements.

Acknowledgments

The first author is ever grateful to Dr. Mauricio Moreno Sereno and Francisco Palacio for their kind support, encouragements, and trust as well as their valuable guidance and discussions on this research project.

References

- [1] D. Grieshaber, R. MacKenzie, J. Voros, and E. Reimhult, "Electrochemical Biosensors-Sensor Principles and Architectures," in *Sensors*. Vol. 8, 2008, pp. 1400-1458.
- [2] Lorena Diéguez Moure, Mauricio Moreno Sereno, "Optical Grating Coupler Bio-sensor and Bio-medical Applications", Barcelona, July 2012.
- [3] Biacore, *BIAtchnology Handbook, version AB*, 1998.
- [4] T. Akimoto, S. Sasaki, K. Ikebukuro, and I. Karube, "Effect of incident angle of light on sensitivity and detection limit for layers of antibody with surface Plasmon resonance spectroscopy," *Biosensors and Bioelectronics*, vol. 15, pp. 355-362, 2000.
- [5] J. G. Quinn, S. O'Neill, A. Doyle, C. McAtamney, D. Diamond, B.D. MacCraith, and R. O'Kennedy, "Development and Application of Surface Plasmon Resonance-Based Biosensors for detection of Cell-Ligand Interactions," *Analytical Biochemistry*, vol. 281, pp. 135-143, 2000.
- [6] Hamid Keshmiri, Mauricio Moreno Sereno, Rosa M. Pinto, "Colorimetric resonant reflectance in photonic crystal biosensor structures," *Maximum Planck Institute for the Science of Light*. 2009-11-13.
- [7] C. Lenaerts ; J. Hastanin ; B. Pinchemel ; S. Maricot ; J.-P. Vilcot ; S. Habraken ; N. Maalouli ; E. Wijaya ; M. Bouazaoui ; C. Desfours ; K. Fleury-Frenette. "Integrated prism-free coupled surface plasmon resonance biochemical sensor." *Proc. SPIE 8424, Nanophotonics IV*, 84240P (April 30, 2012); doi:10.1117/12.922579.
- [8] <http://www.owls-sensors.com/OWLS-System>
- [9] www.microvacuum.com
- [10] Nasser Darwish, Mauricio Moreno Sereno, "Optical Biosensing with Nanostructured Surfaces," 09/2011
- [11] <http://www.hamamatsu.com/eu/en/product/alpha/N/4120/S3922-128Q/index.html>
- [12] <http://www.alldatasheet.com/datasheetpdf/pdf/517251/MICROCHIP/PIC24HJ64GP502.html>
- [13] <http://www.ftdichip.com/Products/Cables/USBTTLSerial.html>